Mild Elevation of Body Temperature Reduces Tumor Interstitial Fluid Pressure and Hypoxia and Enhances Efficacy of Radiotherapy in Murine Tumor Models

Arindam Sen[1], Maegan L. Capitano[1], Joseph A. Spernyak[2], John T. Schueckler[1], Seneca Thomas[1], Anurag K. Singh[3], Sharon S. Evans[1], Bonnie L. Hylander[1], and Elizabeth A. Repasky[1]

Abstract

Human and rodent solid tumors often exhibit elevated interstitial fluid pressure (IFP). This condition is recognized as a prognostic indicator for reduced responses to therapy and decreased disease-free survival rate. In the present study, we tested whether induction of a thermoregulatory-mediated increase in tissue blood flow, induced by exposure of mice to mild environmental heat stress, could influence IFP and other vascular parameters within tumors. Using several murine tumor models, we found that heating results in a sustained reduction in tumor IFP correlating with increased tumor vascular perfusion (measured by fluorescent imaging of perfused vessels, laser Doppler flowmetry, and MRI) as well as a sustained reduction in tumor hypoxia. Furthermore, when radiation therapy was administered 24 hours postheating, we observed a significant improvement in efficacy that may be a result of the sustained reduction in tumor hypoxia. These data suggest, for the first time, that environmental manipulation of normal vasomotor function is capable of achieving therapeutically beneficial changes in IFP and microvascular function in the tumor microenvironment. *Cancer Res; 71(11); 3872–80. ©2011 AACR.*

Introduction

Tumor blood vessels often lack adequate smooth muscle coverage and exhibit both defective vasomotor activity and increased permeability (1–3). This creates a microenvironment in which fluid accumulation and increased protein concentration (resulting in increased oncotic pressure; ref. 4) contribute significantly to elevated interstitial fluid pressure (IFP; refs. 5, 6). The degree of elevation differs both between tumors and, regionally, within tumors. Patient tumors and human tumor xenografts exhibit IFPs ranging from a minimum of 2.6 mm Hg to a maximum of 40 mm Hg, in contrast to the IFP of normal tissue which is typically between -3 and $+3$ mm Hg (5, 7–9). Although there are fewer studies on IFP measurements in murine tumor models, the values reported are elevated, ranging from 3.6 to 15 mm Hg (10–12).

Two decades previously, it was recognized that elevated IFP could impede delivery of therapeutics into tumors (13) and, currently, the challenge involved in the delivery of therapeutic drugs and antibodies into interior tumors is clearly understood (5, 9, 14). Interestingly, cytotoxic drugs [diphtheria toxin

(15), taxanes (10), and paclitaxel (16)], which kill tumor cells directly, may decompress tumors leading to improved tumor vascular function as well as decreased tumor IFP (10, 16). Consistent with these observations, there is a recent report showing that, following chemotherapy, early decrease in IFP is predictive of a better tumor response (12). Furthermore, elevated IFP compromises the response of tumors to radiotherapy (3, 17). Because hypoxia is clearly related to radioresistance, it has been proposed that the abnormal vascularization of tumors leads to increased hypoxia whereas reperfusion could improve radiosensitivity of tumors (18) Recently, it was reported that, in a head and neck xenograft model, treatment with the EGFR (epidermal growth factor receptor) inhibitor erlotinib led to decreased HIF-1α (hypoxia-inducible factor 1 α) and VEGR expression, which, in turn, led to vascular normalization, improved blood flow, increased oxygenation, and improved response to radiotherapy (19). However, whether IFP was altered by erlotinib was not evaluated in this study. Importantly, pretreatment IFP has also been shown to be an independent prognostic factor determining the survival rate of patients with cervical cancer treated with radiotherapy (8). Furthermore, using a human melanoma xenograft model, it was determined that, whereas IFP was variable within a cohort of tumors, tumors with lower IFP displayed better response to subsequent radiotherapy (20). These data associating lower IFP with improved response to radiotherapy support the need to identify strategies that can safely reduce tumor IFP.

Cancer researchers have, for a long time, been interested in the radiosensitizing effects obtained by local delivery of heat

Authors' Affiliations: Departments of [1]Immunology, [2]Animal Resources, and [3]Radiation Oncology, Roswell Park Cancer Institute, Buffalo, New York

Corresponding Author: Elizabeth A. Repasky, Department of Immunology, Roswell Park Cancer Institute, Buffalo, NY 14263. Phone: 716-845-3133; Fax: 716-845-8552; E-mail: elizabeth.repasky@roswellpark.org

*American Association for **Cancer Research***

to tumors, with the goal of achieving cytotoxic temperatures between 42°C and 45°C (21–23), a range which can kill tumor cells and destroy the vascular endothelium. However, other work has revealed that local heat treatments at milder temperatures, between 39°C and 42°C, can improve oxygenation of tumors and vascular perfusion, and result in radiosensitization (reviewed in refs. 24–27). Works by other researchers (28, 29) and ourselves (30) have shown positive antitumor effects induced by using mild systemic heating at physiologically achievable temperatures (39°C–39.5°C). In the present study, both normal and tumor tissues are heated, raising the possibility (31) that homeostatic, thermoregulatory mechanisms designed to control core body temperature could have been engaged (31, 32). Because our initial studies revealed that the microvasculature of experimental murine tumors (but not normal organs) exhibited evidence of improved perfusion which persisted well beyond the period of heating of the mice (30, 33), we decided to explore whether these thermally induced vascular changes could affect tumor IFP. Using 3 murine models, we found that mild systemic heating significantly reduced tumor IFP and that this effect was sustained for at least 24 hours postheating. Importantly, this effect correlated with increased vascular perfusion, a reduction in tumor hypoxia, and a significant improvement in response to radiotherapy. Collectively, our data support the hypothesis that targeting normal, thermoregulatory vasomotor function results in therapeutically beneficial changes in the tumor microenvironment.

Materials and Methods

Animal models

The murine colon tumor 26 (CT26) in BALB/c mice and murine melanoma B16.F10 in C57BL/6 mice were grown by s.c. injection of 1×10^6 cells; murine mammary 4T1 tumors were grown by injection of 1×10^6 cells in the mammary fat pads of female BALB/c mice. Tumor volume was determined using the formula, volume $=$ width^2 $\times$ length/2. Animal studies were approved by the Roswell Park Cancer Institute (Buffalo, NY) Animal Care and Use Committee. Mice were obtained from the National Cancer Institute (NCI-NIH). All cell lines were obtained from the American Type Culture Collection.

Whole-body heating

Body temperature of mice was raised using an environmental chamber (Memmert model BE500), as described previously (30). Sentinel mice (1 per cage) were s.c. implanted with temperature transponders near the shoulder (BioMedic Data Systems, Inc.) 2 days before heating. The transponder reading ("body temperature") is typically within ±0.1°C of the core temperature measured by rectal probe (33). Mice were injected with 1 mL sterile saline, intraperitoneally (i.p.), to prevent dehydration, and then placed in a cabinet at room temperature (22°C) or in preheated cages (38.5°C) in the incubator. Temperatures of sentinel mice were recorded initially every 30 to 45 minutes for the duration of the heating.

IFP measurement

IFP was measured by a modified "wick-in-needle" technique using custom-designed instrumentation based on a published design (11). Measurements were made with a MikroTip catheter transducer (model SPR-524; Millar Instruments) via a 23.5-gauge wing-tipped needle. The transducer was interfaced to a PC using a pressure control unit (PCU-2000; Millar Instruments) via an USB analog-to-digital converter (model DT9816; Data Translation). The software used to acquire the data was developed in our laboratory using DT Measure Foundry (version 4.0.7; Data Translation). The needle was inserted into the tumor and measurements were taken every few millimeters along the entry path and averaged. The instrument was calibrated using a custom-built water-column manometer.

Detection of perfused blood vessels

To visualize perfused blood vessels, 50 μL of 0.4 mg/mL fluorescent dye DiOC$_7$(3) [in 75% dimethyl sulfoxide (DMSO); ref. 34] was administered via tail vein 2 hours after heating; 30 seconds later, the animal was sacrificed. Tumors and muscle were resected, embedded in Tissue-Tek OCT (QIAGEN), and 6- to 10-μm-thick sections were cut. Images were recorded and DiOC$_7$ profiles were counted manually or using a particle analysis routine in NIH Image J (NIH). The total number of blood vessels was visualized using rat anti-mouse CD31 antibody (Becton Dickinson Pharmingen; clone MEC13.3).

Tumor blood-flow measurements

Tumor blood flow was measured by laser Doppler flowmetry using OxyFlo (Oxford Optronix Inc.) fitted with a surface probe. Hair was removed 24 hours before measurements. Measurements were made in independent groups of unheated controls or in mice 2 hours after heating by using probes at 5 different locations on the tumor surface. A series of 5 measurements at each site was recorded and averaged to determine blood flow within the tumor in blood perfusion units (BPU).

Determination of fractional vascular volume by MRI using albumin-(Gd-DTPA)$_{35}$

Image acquisition. The change in fractional vascular volume of intratumoral vessels in response to heating was monitored using contrast-enhanced MRI (35, 36). CT26 cells were s.c. implanted, either unilaterally or bilaterally, in the hind legs of BALB/c mice and grown to a volume of 200 to 400 mm^3 before being imaged. These tumor volumes were used to ascertain adequate sampling of tumor-associated voxels and to reduce possible artifacts from differences in magnetic susceptibility between air and tumor tissue. A group of mice (10 tumors) underwent heating, were acclimated to room temperature for 1 hour, and then imaged; untreated control mice (9 tumors) were not heated. Imaging was done on a 4.7-T MRI system using a 35-mm transceiver coil (Broker Biospin). Anesthesia was maintained during imaging with 2% to 3% isoflurane, and animal temperature and respiration were monitored and maintained using a physiologic monitoring system (model 1025; SA Instruments). Following scout scans, 3 baseline R_1 ($1/T_1$ time) measurements were acquired using a fast spin-echo, saturation recovery method with variable

repetition times (TR = 360–6,000 milliseconds). Additional scan parameters were as follows: effective echo time = 20 milliseconds, field-of-view = 32 × 32 mm, matrix size = 128 × 96, slice thickness = 1 mm, averages = 1, acquisition time = 5 minutes. Following baseline R1 measurements, mice were injected, via tail vein, with albumin-(Gd-DTPA)$_{35}$ (Contrast Media Laboratory, USFC, San Francisco, CA) at a concentration of 0.1 mmol/kg. A 3-dimensional angiographic scan was acquired to confirm the quality of the injection and then serial R_1 measurements were obtained for up to 45 minutes postinjection.

Image analysis. Regions of interest (ROIs) for tumor and back muscle were drawn using commercially available software (Analyze 7.0; AnalyzeDirect). Average signal intensities at each TR were determined within each ROI, and the R_1 values were calculated by nonlinear fitting of the equation: $S_{TR} = S_{MAX}[1 - e^{-(R_1 \cdot TR)}]$ using Matlab (Matlab 2008a; MathWorks Inc.). The increase in R_1 (ΔR_1), which is proportional to contrast agent concentration, was calculated by subtracting the average baseline R_1 value from each postinjection value. To account for injection variability, ΔR_1 values for the tumor were normalized by dividing the ΔR_1 of the back muscle. Fractional vascular volumes of the tumors were obtained from the y-intercept of a linear regression fit of ΔR_1 versus time-elapsed postinjection (37). A single data point in the control group was deemed an outlier by the extreme studentized deviate method ($P < 0.05$) and excluded from statistical analysis. T_1 relaxation rate parameter maps were calculated from the first T_1 measurement acquired after contrast agent injection on a pixel-by-pixel basis. To determine the increase in R_1, the preinjection T_1 rate of the tumor was subtracted from the generated R_1 map. The ΔR_1 maps were then normalized by dividing by the mean ΔR_1 of back muscle. A color lookup table was applied to the ratio maps and overlaid upon black and white anatomic images.

Hypoxyprobe-1 administration and immunohistochemistry

Pimonidazole hydrochloride (60 mg/kg) was administered i.p. at 2, 24, and 48 hours postheating. Tumors were collected 45 minutes postinjection (according to manufacturer's instructions), fixed in 10% formalin, and embedded in paraffin. Immunohistochemistry was carried out on 6- to 10-μm-thick paraffin sections using the Hypoxyprobe-1 Plus Kit (Chemicon International HP2-100), according to the manufacturer's instructions. Brightfield images were acquired using a SPOT-2 camera and SPOT Advanced Version 3.5.9.1 Software (Diagnostic Instruments, Inc.).

Local radiation treatment

Animals were heated 24 hours before the first radiation treatment. CT26 tumor–bearing mice received 4 Gy of radiation, fractionated over 4 days at the rate of 1 Gy/d. B16.F10 tumor–bearing mice received 20 Gy of radiation, fractionated over 5 days at the rate of 4 Gy/d. Initial tumor volumes measured were 120 to 130 mm^3. For radiation treatment, the mice were anesthetized with isoflurane (induction at

3%–5%; maintenance at 1%–2%). Mice were shielded with 2-mm-thick lead plates with small apertures limiting exposure to the tumors. Radiation was carried out with an orthovoltage X-ray machine (Philips RT250; Philips Medical Systems) at 75 kV using a 1 × 2-cm cone. Experiments were concluded when mice had to be removed from a group because of large tumor volume (~1,500 mm^3) or because of tumor ulceration.

Statistics

ANOVA with Dunnett's multiple comparison tests was used for comparatively analyzing the means of multiple treatment groups to that of a control untreated group; Student's t test was used for comparing the means of only 2 groups. Significant statistical differences between the unheated control group and the treated groups are labeled as *, **, and *** for $P < 0.05$, <0.01, and <0.001, respectively.

Results

Tumor IFP is reduced after heating

Mice bearing CT26 tumors (300–600 mm^3) were heated to 39.5°C for 6 hours and then returned to an environment at room temperature (~21°C–22°C); control mice were unheated. IFP measurements were taken at 2 hours postheating. A third group received 2 doses of paclitaxel (30 mg/kg; 48 hours apart), a treatment shown to reduce tumor IFP (16), and IFP was measured 24 hours after the second dose. We observed a significant reduction of tumor IFP in animals heated for 6 hours (1.27 ± 0.49 vs. 3.37 ± 0.45 cm H$_2$O in controls; $P < 0.05$), although there was a range in the IFP values of tumors within each group (Fig. 1A) and this reduction was comparable with that resulting from paclitaxel treatment (1.6 ± 0.24 cm H$_2$O). Similar results were obtained when mice bearing B16.F10 tumors were heated for 6 hours (Fig. 1B; 5.93 ± 0.6 cm H$_2$O in control group vs. 3.7 ± 0.23 cm H$_2$O in mice at 2 hours postheating and 2.83 ± 0.34 cm H$_2$O in mice at 24 hours postheating; $P < 0.01$).

To determine both the kinetics and durability of IFP reduction, a time-course study was conducted. Tumor-bearing mice were heated to 39.5°C for 2, 4, and 6 hours. In CT26, a significant reduction in tumor IFP was achieved by 2 hours of heating (Fig. 1C). Furthermore. we found that after a 6-hour heat treatment, the drop in IFP lasted for at least 24 hours (Fig. 1C). In orthotopically implanted mammary 4T1 tumors, the effect of heating was comparable with that in the subcutaneous models (Fig. 1D). Collectively, these results show that a temporary increase in body temperature results in a significant reduction in tumor IFP which was observed to be maintained at 24 hours postheating in CT26 and B16.F10. The measured IFPs for the murine tumors used in this study are all within the range of IFPs that have been reported in the literature for several tumor models.

Tumor vascular perfusion increases after heating

To determine whether heating (and reduced IFP) also alters vascular perfusion, we evaluated the effect of heating on distribution of a fluorescent dye within tumors vessels. Heated and unheated mice bearing CT26 tumors were injected with
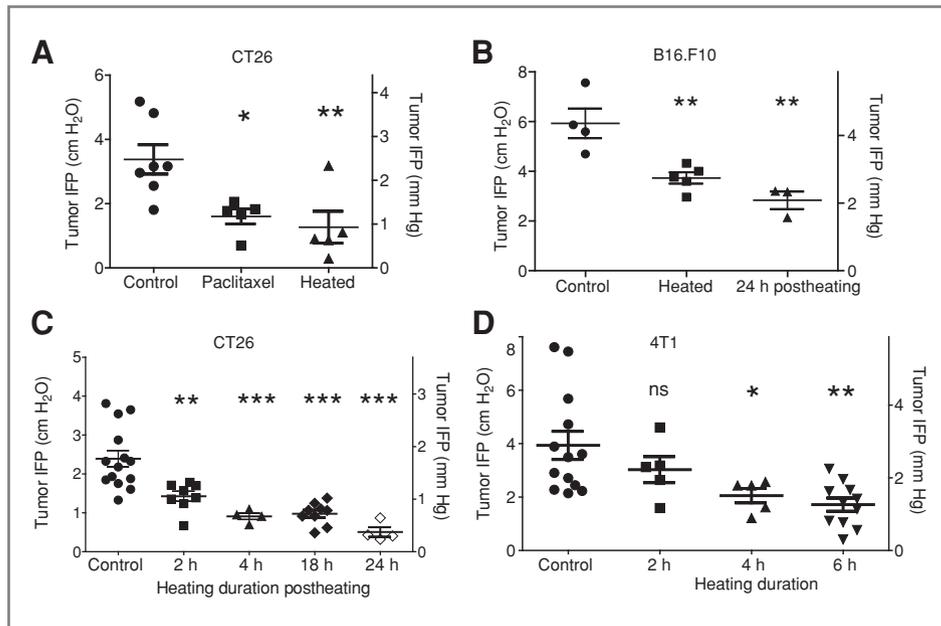
Figure 1. An increase in core body temperature decreases tumor IFPs in syngeneic tumors in BALB/c (CT26 and 4T1) and in C57BL/6 (B16.F10) mice. Heated mice bearing tumors (volume = 300–600 mm^3) were maintained at 39.5°C for specified duration, returned to room temperature for 2 hours, and then IFP measurements were done. Each data point represents the average of multiple measurements in a single tumor. A, CT26 tumors implanted s.c. on the hind leg: IFP of tumors in control untreated mice compared with IFP of tumors in mice treated with either 2 doses of paclitaxel (30 mg/kg) or heat treatment. B, B16. F10 tumors implanted s.c. on the flank: IFP of tumors in control untreated mice compared with IFP of tumors in mice heated to 39.5°C for 6 hours. C, CT26 tumors implanted s.c. on the hind leg: IFP of tumors in control mice compared with IFP of tumors in mice after 2 or 4 hours of heating and 18 and 24 hours after a 6-hour heating treatment. D, 4 T1 tumors implanted orthotopically in the fourth mammary fat pad (volume = 300—600 mm^3). IFP of tumors in control mice and of tumors in mice following 2, 4, or 6 hours of heating. IFP measurements are given in both cm H$_2$O and mm Hg. ANOVA with Dunnett's multiple comparison test was used to evaluate statistical difference between the mean of the control group and the means of the treated groups. *, $P < 0.05$; **, $P < 0.01$; ***, $P < 0.001$; ns, not significant.

DiOC$_7$(3), and the number of vessels perfused by the dye was counted. Overall, a significant increase in perfused vessels was observed following heating, although, again, there was a range of response. A visual comparison of representative sections (Fig. 2A) shows that a tumor from a heated mouse has approximately twice the number of labeled vessels as does a tumor from an unheated mouse (160 vs. 82). Interestingly, normal tissue (skeletal muscle) shows no difference in perfusion (Fig. 2A). Quantification of vessels shows that, while there is a near doubling of DiOC$_7$-perfused vessels (3) in tumor sections from heated mice, there is no change in the number of CD31$^+$ vessels in the same section (Fig. 2B). This suggests that heating results in opening of a large fraction of previously unperfused vessels.

The reduction in IFP following heating correlates with an increase in blood flow

To test whether decreased IFP following heating correlates with increased tumor blood flow, both IFP and tumor blood flow were measured in an unheated control and a heated group of CT26 tumor–bearing mice. For each tumor, blood-flow (laser Doppler flowmetry) measurements were taken first, followed by IFP measurements. The results (Fig. 3A and B) show that decreased IFP is correlated with increased blood flow and that these differences are statistically significant.

The increase both in the number of perfused vessels and in blood flow in tumors would be expected to consequently increase the fractional vascular volume of tumors when determined using macromolecular contrast-enhanced MRI. Pseudo-colorized perfusion maps of CT26 tumors overlaid upon anatomic images from representative mice are shown in Figure 3C; the top panels show perfusion maps from 4 control mice and the bottom panels show perfusion maps of tumors from heated mice. The degree of perfusion is color coded such that red indicates greater perfusion. A 6-fold difference in the ratio of the fractional vascular volume to muscle was observed in tumors of the heated group ($n = 10$) versus that of the control group ($n = 8$; Fig. 3D).

Hypoxia in tumors is reduced by heating

To determine whether increased blood flow in tumors following heating is associated with reduced hypoxia, we visualized changes in tumor hypoxia by immunohistochemical analysis of Hypoxyprobe-1 (pimonidazole hydrochloride; Chemicon International Inc.) localization. The severity of hypoxia present in sections of tumors from unheated mice and in mice at 2, 24, and 48 hours postheating was scored (Fig. 3E). At 2 hours postheating, the degree of hypoxia was greatly reduced compared with unheated tumors; there was some increase in hypoxia at 24 and 48 hours postheating (Fig. 3F). These data indicate that heating results in a
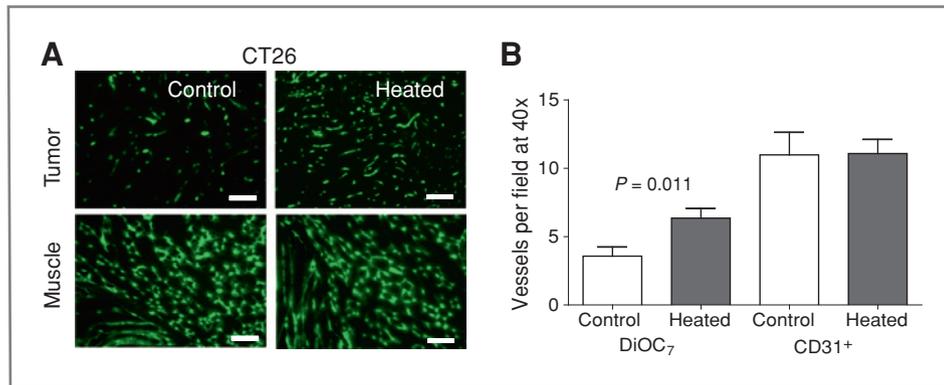
Figure 2. Elevated body temperature increases tumor blood vessel perfusion in BALB/c mice bearing CT26 tumors. A, representative fluorescence micrographs (at 5×) of CT26 tumor implanted s.c. on the hind leg (volume = 300–600 mm³; top pair) and muscle (bottom pair) showing perfused blood vessels following tail vein injection of the cyanine dye DiOC₇(3). The micrographs on the left are those obtained from tissue excised from unheated control mice and the 2 micrographs on the right are from mice after 6 hours of heating. The increased number of perfused vessels in a tumor from a heated mouse (160 vessels per field) is apparent in comparison with that of an untreated mouse (82 vessels per field). There is no visible difference in the number of perfused vessels in muscles from unheated control mice and that from heated animals. B, the average total number of perfused, DiOC₇(3)-labeled blood vessels in tumors from unheated control mice and those from heated mice showing doubling in the number of perfused vessels. The average numbers of anatomic CD31⁺ vessels are not altered by heating. Scale bars, 500 μm.

reduction in tumor hypoxia, with the effect lasting for 24 hours posttreatment.

The efficacy of radiation therapy is enhanced by heating

We next asked whether the reduced IFP, increased vascular perfusion, and decreased hypoxia observed following heating could improve efficacy of subsequent radiation treatment. To test this, CT26 tumor–bearing mice were divided into 4 groups (average size 120–130 mm³): (i) unheated control; (ii) heating only (day 11); (iii) fractionated radiation (1 Gy/d for 4 days, days 12–15); and (iv) 6 hours of heating (39.5°C) followed, 1 day later, by fractionated radiation (Fig. 4A). Heat treatment was given 24 hours before radiation, based on previous findings (Fig. 1) that IFP levels are at their lowest at this time point and based on preliminary studies (data not shown) in which there was no indication of improvement if radiation was given on the same day as heating. Tumors in the unheated and heated-only groups grew at a similar rate and were terminated on day 22 on the basis of tumor size (volume > 1,500 mm³). The growth of tumors in mice receiving only radiation was moderately inhibited. However, growth of tumors in mice that were heated and then subjected to radiation was significantly inhibited, and this effect was maintained for the duration of the experiment.

Similar results were obtained with B16.F10 tumor–bearing mice. Again, mice were divided into 4 groups (average tumor size 100–150 mm³; $n = 5$): (i) unheated control; (ii) heating only (day 10); (iii) fractionated radiation (4 Gy/d for 5 days, days 11–15); and (iv) heating followed by fractionated radiation. As with the CT26 tumors, tumors in the unheated and heated groups grew at the same rate (Fig. 4B). Although tumor growth in the group that received radiation only and the group treated by heating followed by radiation was inhibited, the growth of tumors in the combination treatment group was statistically significantly reduced compared with tumors trea-

ted with radiation alone beginning at day 22. Each of these experiments was repeated with similar outcomes (data not shown).

Discussion

Thermoregulation is essential for maintaining core temperature when the system is faced with environmental or metabolic thermal stress. This regulation is achieved by systemic modulation of cardiovascular function, resulting in actively regulated vasodilation and vasoconstriction of blood vessels (31, 32, 38, 39). Because this regulation is controlled by innervation of smooth muscle and other cells associated with the normal vasculature, which many tumor vessels lack, tumor vessels are not likely to respond to thermoregulatory stimuli in the same way as normal vessels. However, in this study, we asked whether the tumor microenvironment might, nonetheless, be affected by thermoregulatory events in the surrounding tissue.

We found that heating mice with tumors can significantly reduce tumor IFP and hypoxia. Furthermore, we observed a significant improvement in the efficacy of radiation therapy administered 24 hours postheating, an effect that may be a result of the sustained reduction in tumor hypoxia. Although the specific cascade of vasomotor activity in normal tissues that leads to changes within the tumor microenvironment is yet to be identified, thermoregulation-mediated increased blood flow in vascular beds proximal and distal to the tumor vasculature may help to, at least temporarily, improve blood flow through the tumor, possibly by drawing excess fluid from tumor stroma. This would, in turn, reduce IFP, decompress tumor vasculature, and allow more blood to traverse the tumor.

Furthermore, the lack of vasomotor control of tumor vasculature may be a critical factor in the duration of the effect that we observed. Following heating, when the body
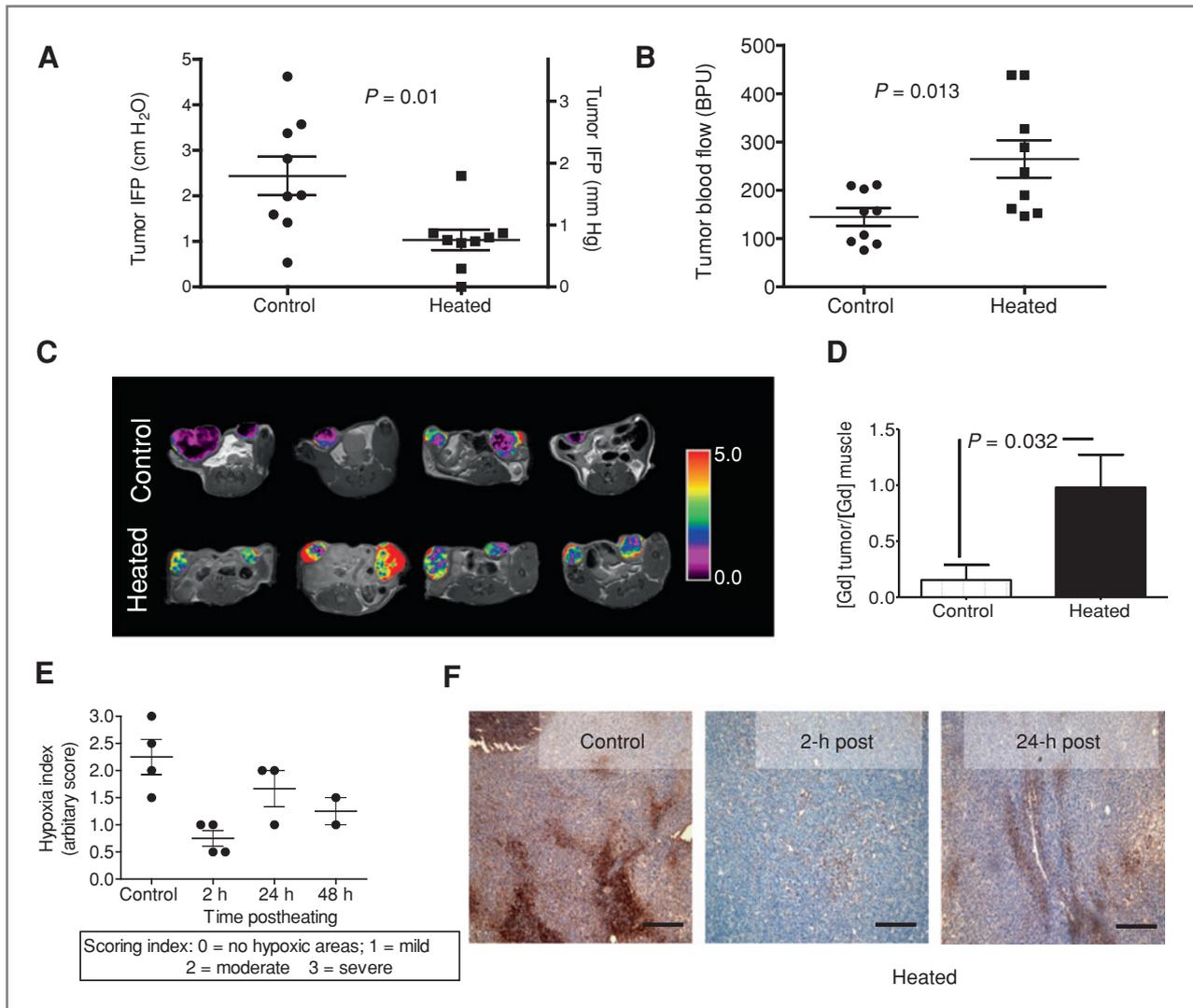
Figure 3. Thermally induced increases in tumor blood flow correlate with decreases in tumor IFP and tissue hypoxia in CT26 tumors. IFP (A) and blood-flow changes (B; as measured by laser Doppler flowmetry) following heating ($n = 9$ per group) of BALB/c mice bearing CT26 tumors implanted s.c. on the flanks (volume = 300–600 mm^3). In these mice, blood flow was measured before IFP measurements were taken. C, changes in blood flow documented by MRI in CT26 tumors implanted s.c. on the hind legs (volume = 200–400 mm^3) following heating: representative pseudo-colorized images of contrast agent enhancement in 4 control animals (top) and another 4 animals following heating (bottom). Tumors in heated animals consistently showed higher amounts of the contrast agent than tumors in control animals, indicating a higher fractional volume of functioning vasculature as a result of heating. Color scale reflects the ratio of the contrast agent in tumors to normal tissue (back muscle). D, plot of the normalized vascular volumes in tumors from unheated control mice and those that were heated. Vascular volumes were determined using a macromolecular MRI contrast agent human serum albumin-Gd-DTPA. Data presented represent the average of each group (control: $n = 8$; heated: $n = 10$). P values are Students' t-test results between the control and the treated data sets. E, scatter-plot of hypoxia index in tumors (s.c. implanted on the flanks; volume = 300–600 mm^3) from untreated mice and treated mice at 2, 24, and 48 hours postheating. F, immunohistochemical localization of pimonidazole hydrochloride (Hypoxyprobe-1) adducts in tumors from control mice and from heated mice at 2 and 24 hours postheating. A reduction in hypoxic areas in the tumor sections (brown staining) following heating can be seen. Scale bars, 500 μm.

temperatures of the mice returned to normal, we observed that increased blood flow in tumors persisted for a period of several hours, whereas in contrast, we found no such sustained changes in the surrounding tissues. This suggests that, among the abnormal properties of tumor vasculature, an apparent, marked limitation in reversible vasomotor control when faced with a temporary challenge to the

thermoregulatory system can be included in that list of defects. However, this defect in tumor vascular perfusion can be exploited to provide a window of time in which access to the tumor microenvironment may be enhanced without further increasing access to normal organs. This suggests that, in addition to improving the efficacy of radiation therapy (as shown here in Fig. 4), mildly preheating animals
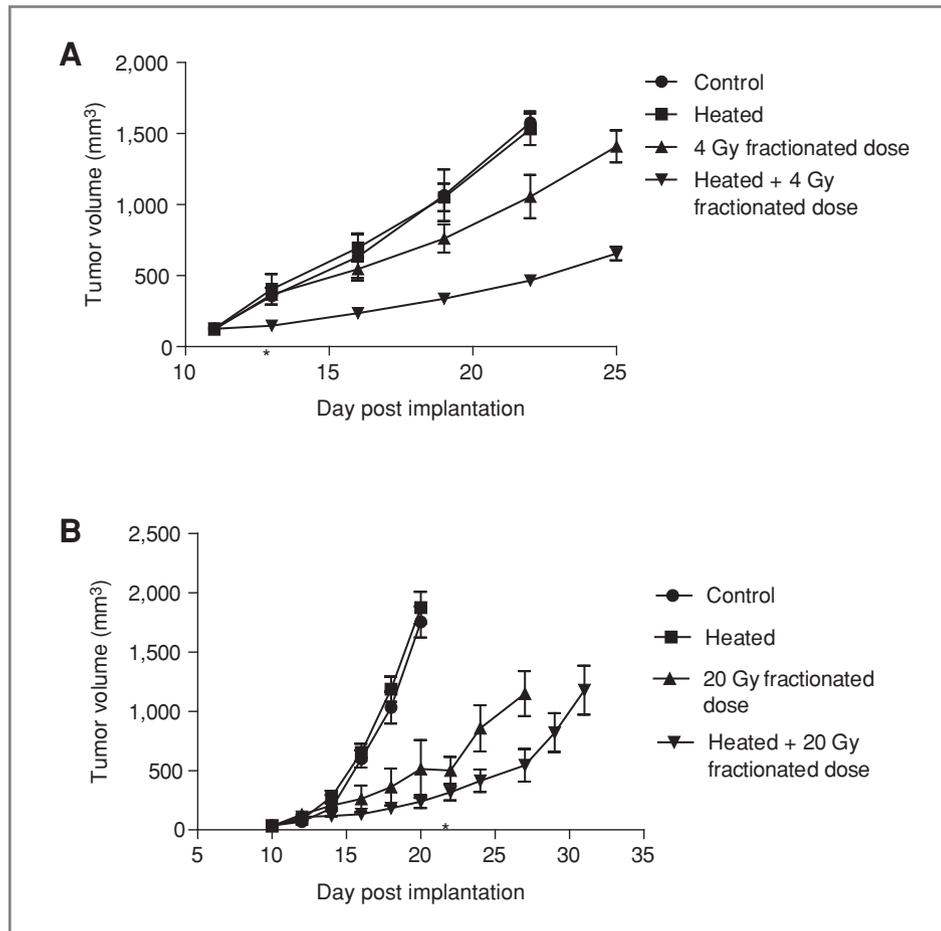
Figure 4. Heat treatment enhances the efficacy of radiation therapy in 2 different tumor models. A, CT26 tumors were implanted s.c. on the flank of BALB/c mice. Tumor growth was then monitored in the following groups ($n = 5$ per group): control untreated mice (●), mice that were only heated (■), mice that received only radiation (1 Gy/d for 4 days, days 12–15; ▲), and mice that were heated and followed 24 hours later by 4 consecutive radiation treatments (1 Gy/d for 4 days, days 12–15; ▼). Tumor growth rates in the unheated control and the heat-only groups were indistinguishable. The slowest growth rate was observed in tumors of mice that received the combination of heating followed by fractionated radiation. Statistical test using one-way ANOVA with Dunnett's multiple comparison test for comparative analysis of the means of the treated groups to the mean of the control group shows significant difference only for the group of mice that received combined heating and radiation. B, B16.F10 tumors were implanted s.c. on the flank of C57BL/6 mice. Kinetics of B16.F10 tumor growth in C57BL/6 mice ($n = 5$), control untreated mice (●), and those that were only heated (day 10; ■), subjected to only radiation (days 11–15; ▲), or subjected to combined radiation and heating (▼). Tumor growth rates in the unheated control and the heating-only groups were comparable. The slowest growth rate was observed in tumors of mice that received fractionated 20 Gy radiation (4 Gy/d) starting 1 day after heating. Tumor volumes in the combined heat and radiation treatment group were significantly smaller ($P < 0.05$) as compared with the radiation-only group from day 24.

may be beneficial for other therapies which depend on improved vascular access to tumors, including chemotherapy, nanoparticles, and antibody therapies, and adoptive cellular immunotherapy. Indeed, in a previous study, we measured a significant increase in the uptake of liposomal doxorubicin following systemic hyperthermia (30) that resulted in improved tumor growth control. Such a strategy could be feasible in humans because an increase in core temperature by less than 1°C results in rapid, cutaneous vasodilation and movement of blood from the core to the skin for heat dissipation (31). Next, it will be important, using these murine preclinical models, to look at deeper seated tumors (e.g., kidney, liver, intestinal tract). Because heat-induced changes in vasomotor activity occur internally also (32, 38–40), it is likely that deeper tumors will also be

significantly impacted by thermal signals. Furthermore, it will be important to study endogenously arising tumors because their vascular properties may be more similar to patient tumors than those of transplantable tumor models.

Because tumors are devoid of neurovascular regulation typical of arteriolar vessels, some pharmacologic agents which can preferentially create vasodilation in the skin or in normal organs have been observed to create conditions resulting in diversion of blood from the tumor to surrounding tissue, or "vascular steal" (ref. 41; reviewed by Jirtle 42), and a reduction in IFP (43). We did not observe a reduction in tumor vascular flow in our study. This may be because thermoregulatory signals, unlike vasodilating drugs (e.g., hydralazine or bradykinin) used for studies on vascular steal (44), result in compensatory vascular events, including constriction of blood vessels in

the core organs, to maintain blood pressure and optimize delivery of heated blood to the skin. However, it is important to note that, in our experiments, at least 1 hour elapsed before we tested blood flow in tumors following heating. It is possible that, during the heating, there may have been transient diversion of blood from the tumor, resulting in reduced IFP which, in turn, ultimately resulted in increased tumor perfusion.

Clinical investigators working in the field of hyperthermic oncology often employ short-term local heating of tumors, usually from an external radiofrequency or ultrasound source, as an adjuvant for cancer therapy (21) and whether IFP is affected by this protocol in patients has not been tested. When we used a local hyperthermia protocol in mice, we did not observe any changes in tumor IFP (unpublished observations), a result which is similar to that reported earlier by other researchers (45). However, in comparing the outcomes of different heating protocols in terms of effects on vasomotor parameters and IFP, it may be very important to consider the heating source, the duration of heating and temperature achieved, and whether general anesthetics are used. A report by Leunig and colleagues (46) using local hyperthermia at 43°C reported a reduction in tumor IFP; however, in that study, the cytotoxic temperature resulted in vascular collapse through rapid endothelial cell death. Furthermore, unlike the protocol used in the present study in which the animals are not restrained or anesthetized, most local hyperthermia experiments on mouse and rat models employ a general anesthetic (e.g., ketamine mixtures) to subdue the animal. Because general anesthetics such as ketamine are known to cause vasoconstriction (47), it is likely that the thermoregulatory responses (and subsequent changes in IFP and vascular perfusion) may be limited.

Whole-body hyperthermia on tumor-bearing rat and mouse models has also been carried out (28, 29, 33) as has whole-body heating in patients (48); however, tumor IFP was not measured in those studies. A recent phase III clinical trial in which patients with high-risk sarcoma (49) were treated with "deep regional" hyperthermia in combination with chemoradiotherapy revealed significant positive benefits. This regional heating protocol, which heats larger volumes of tissue in comparison with local hyperthermia, may also engage thermoregulatory responses. However, measurements of IFP or intratumoral vascular perfusion were not conducted in this trial. Acquiring this information will be an exciting opportunity to understand better the clinical benefits that can be achieved with various hyperthermia protocols.

In summary, in this study we show that mild warming of mice results in noncytotoxic, highly physiologically relevant changes in the tumor microenvironment, providing a potential window of time in which improved vascular access to the tumor can be achieved for therapy. Exploiting thermoregulation has the attractive feature of being more universally applicable than many other approaches and could be easily combined with other therapies, thus reducing exposure to cytotoxic drugs. An intriguing possibility is that sustained exercise, known to stimulate many of the same thermoregulatory responses as by increased ambient temperature (31, 50) may also have a positive effect on reducing tumor IFP. Collectively, these results provide a strong rationale for exploiting normal thermoregulatory responses to improve efficacy of therapies that are dependent on vascular perfusion and compromised by high intratumoral pressures.

Disclosure of Potential Conflicts of Interest

No potential conflicts of interest were disclosed.

References

1. Jain RK. Barriers to drug delivery in solid tumors. Sci Am 1994; 271:58–65.
2. Dvorak HF. How tumors make bad blood vessels and stroma. Am J Pathol 2003;162:1747–57.
3. Vaupel P. Tumor microenvironmental physiology and its implications for radiation oncology. Semin Radiat Oncol 2004;14:198–206.
4. Stohrer M, Boucher Y, Stangassinger M, Jain RK. Oncotic pressure in solid tumors is elevated. Cancer Res 2000;60:4251–5.
5. Heldin CH, Rubin K, Pietras K, Ostman A. High interstitial fluid pressure—an obstacle in cancer therapy. Nat Rev Cancer 2004;4: 806–13.
6. Fukumura D, Jain RK. Tumor microvasculature and microenvironment: targets for anti-angiogenesis and normalization. Microvasc Res 2007;74:72–84.
7. Roh HD, Boucher Y, Kalnicki S, Bauchsbaum R, Bloomer WD, Jain RK. Interstitial hypertension in carcinoma of uterine cervix in patients: possible correlation with tumor oxygenation and radiation response. Cancer Res 1991;51:6695–8.
8. Milosevic MMD, Fyles AMD, Hill RPP. Interstitial fluid pressure in cervical cancer: guide to targeted therapy. Amer J Clin Oncol 2001; 24:516–21.
9. Lunt SJ, Kalliomaki TMK, Brown A, Yang VX, Milosevic M, Hill RP. Interstitial fluid pressure, vascularity and metastasis in ectopic, orthotopic and spontaneous tumours. BMC Cancer 2008;8:2.
10. Griffon-Etienne G, Boucher Y, Brekken C, Suit HD, Jain RK. Taxane-induced apoptosis decompresses blood vessels and lowers interstitial fluid pressure in solid tumors: clinical implications. Cancer Res 1999;59:3776–82.
11. Ozerdem U, Hargens AR. A simple method for measuring interstitial fluid pressure in cancer tissues. Microvasc Res 2005;70:116–20.
12. Ferretti S, Allegrini PR, Becquet MM, McSheehy PMJ. Tumor interstitial fluid pressure as an early-response marker for anticancer therapeutics. Neoplasia 2009;11:874–81.
13. Jain RK. Transport of molecules across tumor vasculature. Cancer Metastasis Rev 1987;6:559–93.

14. Minchinton AI, Tannock IF. Drug penetration in solid tumours. Nat Rev Cancer 2006;6:583–92.

15. Padera T, Stoll BR, Tooredman JB, Capen D, Di Tomaso E, Jain RK. Cancer cells compress intratumor vessels. Nature 2004;427:695.

16. Taghian AG, Abi-Raad R, Assaad SI, Casty A, Ancukiewicz M, Yeh E, et al. Paclitaxel decreases the interstitial fluid pressure and improves oxygenation in breast cancers in patients treated with neoadjuvant chemotherapy: clinical implications. J Clin Oncol 2005; 23:1951–61.

17. Lee CG, Heijn M, Di Tomaso E, Griffon-Etieene G, Ancukiewicz M, Koike C, et al. Anti-vascular endothelial growth factor treatment augments tumor radiation response under normoxic or hypoxic conditions. Cancer Res 2000;60:5565–70.

18. Moeller BJ, Richardson RA, Dewhirst MW. Hypoxia and radiotherapy: opportunities for improved outcomes in cancer treatment. Cancer Metastasis Rev 2007;26:241–8.

19. Cerniglia GJ, Pore N, Tsai JH, Schultz S, Mick R, Choe R, et al. Epidermal growth factor receptor inhibition modulates the microenvironment by vascular normalization to improve chemotherapy and radiotherapy efficacy. PLoS One 2009;4:e6539.

20. Rofstad EK, Ruud EBM, Mathiesen B, Galappathi K. Associations between radiocurability and interstitial fluid pressure in human tumor xenografts without hypoxic tissue. Clin Cancer Res 2010; 16:936–45.

21. Viglianti BL, Stauffer P, Repasky E, Jones E, Vujaskovic A, Dewhirst M Hyperthermia. In: Hong W, Bast R Jr, Hait W, Kufe DW, Holland JF, Pollock RE, et al., editors. Holland-Frei Cancer Medicine. 8th ed. Shelton, CT: People's Medical Publishing House-USA; 2010. p. 528–40.

22. Corry PM, Dewhirst MW. Thermal medicine, heat shock proteins and cancer. Int J Hyperthermia 2005;21:675–7.

23. Roti Roti JL. Cellular responses to hyperthermia (40–46°C): cell killing and molecular events. Int J Hyperthermia 2008;24:3–15.

24. Griffin RJ, Dings RPM, Jamshidi-Parsian A, Song CW. Mild temperature hyperthermia and radiation therapy: role of tumour vascular thermotolerance and relevant physiological factors. Intl J Hyperthermia 2010;26:256–63.

25. Vaupel PW, Kelleher DK. Pathophysiological and vascular characteristics of tumours and their importance for hyperthermia: heterogeneity is the key issue. Int J Hyperthermia 2010;26:211–23.

26. Song CW, Park H, Griffin RJ. Improvement of tumor oxygenation by mild hyperthermia. Radiat Res 2001;155:515–28.

27. Vujaskovic Z, Song CW. Physiological mechanisms underlying heat-induced radiosensitization. Int J Hyperthermia 2004;20:163–74.

28. Sakaguchi Y, Makino M, Kaneko T, Stephens LC, Strebel FR, Danhauser LL, et al. Therapeutic efficacy of long duration-low temperature whole body hyperthermia when combined with tumor necrosis factor and carboplatin in rats. Cancer Res 1994;54:2223–7.

29. Sakaguchi Y, Stephens LC, Makino M, Kaneko T, Strebel FR, Danhauser LL, et al. Apoptosis in tumors and normal tissues induced by whole body hyperthermia in rats. Cancer Res 1995;55:5459–64.

30. Xu Y, Choi J, Hylander B, Sen A, Evans SS, Kraybill WG, et al. Fever-range whole body hyperthermia increases the number of perfused tumor blood vessels and therapeutic efficacy of liposomally encapsulated doxorubicin. Int J Hyperthermia 2007;23:513–27.

31. Guyton A, Hall J. Body temperature, temperature regulation and fever. Text book of medical physiology. 11th ed. Philadelphia, PA: Elsevier Inc.; 2006. p. 889–900.

32. Gordon C. Thermoregulatory effector responses. Body temperature. Temperature regulation in laboratory rodents. New York, NY: Cambridge University Press; 1993. p. 73–134.

33. Burd R, Dziedzic TS, Xu Y, Caligiuri MA, Subjeck JR, Repasky EA. Tumor cell apoptosis, lymphocyte recruitment and tumor vascular changes are induced by low temperature, long duration (fever-like) whole body hyperthermia. J Cell Physiol 1998;177:137–47.

34. Trotter MJ CD, Olive PL. Use of a carbocyanine dye as a marker of functional vasculature in murine tumours. Br J Cancer 1989;59:706–9.

35. Bhujwalla ZM, Artemov D, Natarajan K, Solaiyappan M, Kollars P, Kristjansen PEG. Reduction of vascular and permeable regions in solid tumors detected by macromolecular contrast magnetic resonance imaging after treatment with antiangiogenic agent TNP-470. Clin Cancer Res 2003;9:355–62.

36. Schmiedl U, Ogan M, Paajanen H. Albumin labeled with Gd-DTPA as an intravascular, blood pool-enhancing agent for MR imaging: biodistribution and imaging studies. Radiology 1987;162:205–10.

37. Bhattacharya A, Toth K, Mazurchuk R, Spernyak JA, Slocum HK, Pendyala L, et al. Lack of microvessels in well-differentiated regions of human head and neck squamous cell carcinoma A253 associated with functional magnetic resonance imaging detectable hypoxia, limited drug delivery, and resistance to irinotecan therapy. Clin Cancer Res 2004;10:8005–17.

38. Gordon C. Influence of heating rate on control of heat loss from the tail in mice. Am J Physiol 1983;244:R778–84.

39. Gordon C. Behavioral and autonomic thermoregulation in mice exposed to microwave radiation. J Appl Physiol 1983;55:1242–8.

40. Charkoudian N. Skin blood flow in adult human thermoregulation: how it works, when it does not, and why. Mayo Clinic Proc 2003;78: 603–12.

41. von Ardenne M. Synergic therapeutic effect of selective local hyperthermia and selective optimized hyperacidity against tumors. Theoretical and experimental bases. Ther Ggw 1977;166:1299–316.

42. Jirtle R. Chemical modification of tumor blood flow. Int J Hyperthermia 1988;4:356–72.

43. Zlotecki RA, Baxter LT, Boucher Y, Jain RK. Pharmacologic modification of tumor blood flow and interstitial fluid pressure in a human tumor xenograft: network analysis and mechanistic interpretation. Microvasc Res 1995;50:429–43.

44. Dewhirst MW, Vinuya RZ, Ong ET, Klitzman B, Rosner G, Secomb TW, et al. Effects of bradykinin on the hemodynamics of tumor and granulating normal tissue microvasculature. Radiat Res 1992;130: 345–54.

45. Hauck ML, Coffin DO, Dodge RK, Dewhirst MW, Mitchell JB, Zalusky MR. A local hyperthermia treatment which enhances antibody uptake in a glioma xenograft does not affect tumor interstitial fluid pressure. Int J Hyperthermia 1997;13:307–16.

46. Leunig M, Goetz AE, Dellian M, Zetterer G, Gamarra F, Jain RK, et al. Interstitial fluid pressure in solid tumors following hyperthermia: possible correlation with therapeutic response. Cancer Res 1992;52: 487–90.

47. Brookes ZLS, Brown NJ, Reilly CS. Intravenous anaesthesia and the rat microcirculation: the dorsal microcirculatory chamber. Br J Anaesth 2000;85:901–3.

48. Bull JM, Scott GL, Strebel FR, Nagle VL, Oliver D, Redwine M, et al. Fever-range whole-body thermal therapy combined with cisplatin, gemcitabine, and daily interferon-alpha: a description of a phase I-II protocol. Int J Hyperthermia 2008;24:649–62.

49. Issels RD, Lindner LH, Verweij J, Wust P, Reichardt P, Schem BC, et al. Neo-adjuvant chemotherapy alone or with regional hyperthermia for localised high-risk soft-tissue sarcoma: a randomised phase 3 multicentre study. Lancet Oncol 2010;11:561–70.

50. McArdle W, Katch F, Katch V. Exercise and thermal stress. Excercise physiology. 7th ed. New York, NY: Wolters Kluwer; 2010. p. 611–38.

Cancer Research

AACR American Association for Cancer Research

Mild Elevation of Body Temperature Reduces Tumor Interstitial Fluid Pressure and Hypoxia and Enhances Efficacy of Radiotherapy in Murine Tumor Models

Arindam Sen, Maegan L. Capitano, Joseph A. Spernyak, et al.

Updated version	Access the most recent version of this article at: doi:10.1158/0008-5472.CAN-10-4482

Cited articles	This article cites 46 articles, 11 of which you can access for free at: http://cancerres.aacrjournals.org/content/71/11/3872.full#ref-list-1
Citing articles	This article has been cited by 6 HighWire-hosted articles. Access the articles at: http://cancerres.aacrjournals.org/content/71/11/3872.full#related-urls

E-mail alerts	Sign up to receive free email-alerts related to this article or journal.
Reprints and Subscriptions	To order reprints of this article or to subscribe to the journal, contact the AACR Publications Department at pubs@aacr.org.
Permissions	To request permission to re-use all or part of this article, use this link http://cancerres.aacrjournals.org/content/71/11/3872. Click on "Request Permissions" which will take you to the Copyright Clearance Center's (CCC) Rightslink site.